

The performance of UVES, the echelle spectrograph for the ESO VLT and highlights of the first observations of stars and quasars

Sandro D'Odorico, Stefano Cristiani, Hans Dekker, Vanessa Hill, Andreas Kaufer, Taesun Kim and Francesca Primas
European Southern Observatory, D-85740 Garching bei München

ABSTRACT

UVES is a dual beam echelle spectrograph installed at the Nasmyth focus of the UT2 telescope (Kueyen) of the ESO VLT since October 1999. It can reach a resolution of 80000 and 115000 in the blue (300-500nm) and red (420-10050 nm) arm, respectively. The instrument is characterized by great stability (~ 100 m/s after correction for temperature variations) and high efficiency (peaking at 25 % over the range 510-660 nm and $>10\%$ over 330-920nm). The smooth operation of both the new telescope and instrument has led to a remarkable number of highly interesting scientific observations during commissioning. Examples of scientific work on these data are presented to illustrate the unique UV efficiency (detection of Beryllium at 313 nm in the spectrum of a metal poor star, studies of the Lyman α forest and metal lines down to $z = 1.7$), the resolving power and high S/N capability (measurement of the lithium isotope ratio) and far red efficiency (abundance of the undepleted Zinc from the $\lambda 202.6$ nm line in a DLA system at $z=3.4$ toward a faint QSO).

Keywords: very large telescopes, echelle spectrograph, chemical abundances, intergalactic medium

1. UVES PERFORMANCE

1.1. Instrument overview

UVES is a dual-beam echelle spectrograph built by ESO (in collaboration with the Trieste Observatory for the control software) for one of the Nasmyth foci of the second 8.2m VLT telescope (Kueyen). The light from the telescope is fed to two separate entrance slits by dichroic and after being dispersed by two large echelle gratings (one per arm) and a grating crossdisperser (two per arm) is focussed by dioptric cameras on two large size, high efficiency CCD detectors. Table 1

Table 1. Overview of the UVES capability

	<u>BLUE ARM</u>	<u>RED ARM</u>
$\lambda\lambda$ range	300-500 nm	420-1100nm
Res. power x slit (nm/pixel)	~ 41400 0.0019 at 450nm	~ 38700 0.0025 at 600nm
Max. Resolution (2 pix sampling)	~ 80000	~ 110000
Throughput	12% at 400nm	17% at 600nm
Limiting Mag. in 90m, S/N=10	18 at 360nm R=58000	19.5 at 600nm R=62000
CCDs	2048x4096 windowed to 2kx3k	4096x4096 (mosaic of two)
Echelle (R4)	41.59 g/mm	31.6 g/mm
Cross Dispersers	CD1 1000g/mm CD2 660g/mm	CD3 600 g/mm CD4 312 g/mm
Pixel(15 μ m)scale: Dispersion direct. Along slit	0.215" \pm 20% 0.25" (CD1 & CD2)	0.155" \pm 20% 0.18" , 0.17" (CD3 & CD4)
Coverage /frame (nm)	85 (CD1) 126 (CD2) in 33 / 31 orders	200 (CD3) 403 (CD4) in 37 / 33 orders

summarizes the characteristics of the main components and the properties of the spectrograph. A detailed description of UVES and its various subsystems is given in Dekker et al.¹ The paper by Dorn et al.² addresses the instrument detector system and the one by Longinotti et al.³ the control system. The instrument definition was completed in May 1994 and UVES saw first light on September 27th, 1999. After two commissioning periods (October and December 1999) and one week of Science Verification observations (see http://www.eso.org/science/ut2sv/UVES_SV.htm), the instrument has started regular operation in visitor and service mode on April 1st, 2000.

1.2. Resolution

UVES was designed to achieve a maximum resolution with two pixel sampling of 80000 in the blue arm and 110000 in the red arm. These values can be reached with a slit width of 0.3 arcsec in the red arm and 0.4 in the blue, or using image slicers which can be remotely inserted in

Fig.1. Plots of the FWHM of the Th lines in pixels and of the resolution as a function of position on the CCDs and of wavelength (one CCD of UVES red arm).

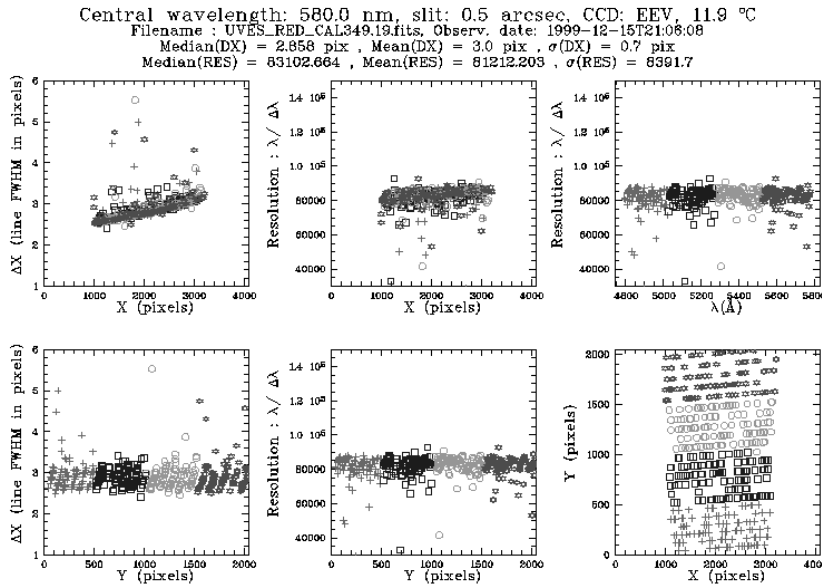
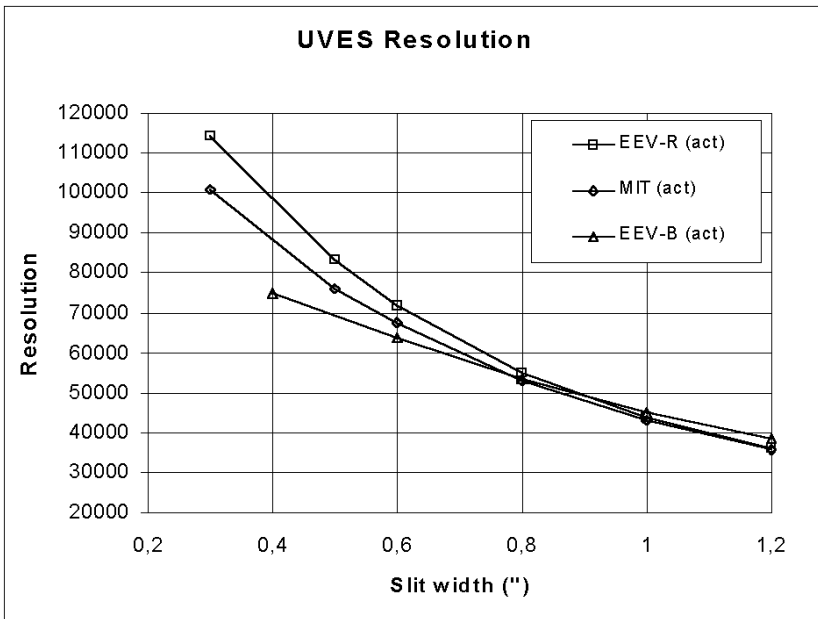


Fig.2 . Resolution measured as a function of slit widths on the blue arm CCD and on the two red arm CCDs (EEV-B, EEV-R and MIT respectively)



phase of UVES it was decided to mount the main optical components on a table bolted to the Nasmyth platform. The stable orientation with respect to gravity was chosen to ensure maximum stability and to relax the constrain on the mass and dimension of the various functions. After the two slit units of the spectrograph, the only moving functions encountered by the optical beams are the cross disperser units and the camera tilt units. The latter can be used to shift the spectra up to ~ 200 pixels in the dispersion direction on the detector, an option that it is not used in standard format observations. Both functions are highly repeatable in positions (better than 0.05 pixel). Observed shifts in the spectra are dominated by the

the focal plane. The full spectral range of the spectrograph (305-1050 nm) can be covered with two single dichroic exposures. A data reduction pipeline is available at the telescope for these standard settings (Ballester et al.⁴). By making use of a physical model of the spectrograph it produces automatic wavelength calibration and extracts the data. Figure 1 (courtesy of O. Boitquin) is a by-product of the pipeline and shows the pixel sampling and the resolving power as a function of the position on the CCD and of wavelength. The first two variables are measured from gaussian fits to the lines of the Thorium wavelength calibration lamp in the different echelle orders. The wavelength calibration is computed automatically by the UVES data reduction pipeline and has typically r.m.s. accuracies of 0.005 Å. The results of this spectral analysis are used to monitor the optical quality of the spectrograph with time. Every standard calibration taken at the telescope is reduced and the results automatically logged in the UVES data base.

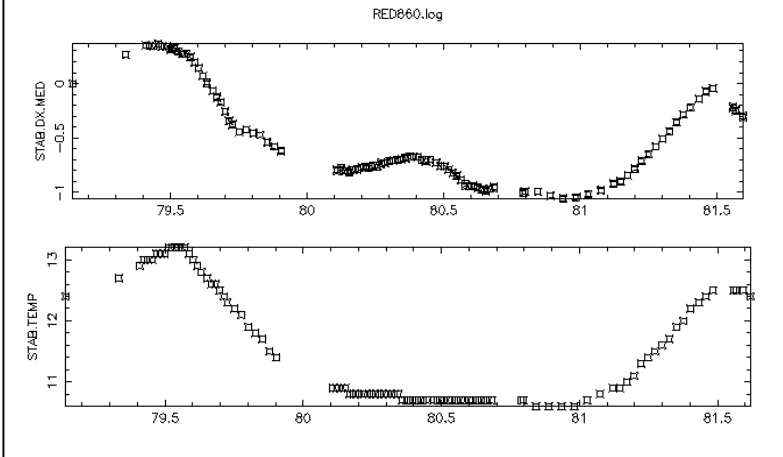
Using spectra taken with different slit widths we derived the resolution/slit relation shown in Fig.2 for the blue and red arm. As the data show, the measured resolution for the MIT/LL CCD in the red mosaic is slightly worse than for the EEV. The MIT/LL chip, at least in the clock setting we operate it, suffers of electron diffusion which results in a larger equivalent pixel size.

1.3. The instrument stability

Early in the concept definition

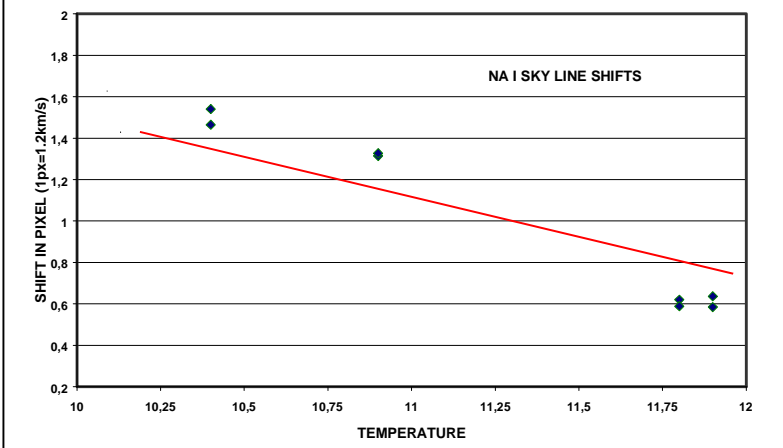
changes induced in the refractive index of the air by temperature variations and to a lesser extent by variations in atmospheric pressure. The FITS headers of the CCD frames include values of the atmospheric pressure and of the temperatures of the air, of the table and of the cameras in the instrument enclosure. It is therefore relatively easy to correlate the variations in the spectral format with these parameters. Figure 3 shows the results of a first test when arc spectra have been taken at regular intervals over a period of two days. The variation of the temperature and the corresponding measured shifts of the spectra of the Thorium lamp in the dispersion direction are well correlated and the relation can be described in

Fig.3. Measured shifts (in pixels) of the spectrum lines in the dispersion direction (upper panel) and of the temperature (lower panel) monitored over a period ~2 days.



velocity accuracy required by the scientific program, the astronomer can decide whether to calibrate the spectrograph with an arc exposure immediately after the science exposure or to request the calibrations to be taken in the following morning.

Fig.4. The line is the preliminary relation between temperature in the UVES enclosure and spectral shifts (in pixels) derived from the Thorium spectra, the filled diamonds are relative positions of sky lines measured in four science exposures taken a few days apart.



Visual-Red spectral ranges in order to optimize the coatings, the dispersive elements (echelle and cross-dispersers) and the detectors. Each cross-disperser unit mounts two gratings back-to-back, to allow for a further optimization within each arm. The CCD detectors are an UV-optimized EEV CCD-44-82 in the blue arm and a mosaic of a standard coating EEV CCD-44-82 and of a MIT/LL CCID-20, all of the 2K x 4K, 15 μm pixel format. The choice of two different CCD types in the mosaic of the red arm was again driven by the desire to use the higher red efficiency device available to us (the MIT/LL chip) for the redder part of our spectral format. Fig.5 shows the most recent efficiency measurements of the telescope-instrument-detector. They are based on observations of two standard stars, with widely open slits and they refer to the top of

first approximation by a line with a slope $\Delta x/\Delta T = 0.4 \text{ pixel/ Degree } ^\circ\text{C}$. We have verified this result by measuring the movement of sky emission lines in spectra taken at different temperatures while the barometric pressure remained almost constant. The results are shown in Fig.4: the shifts are in agreement with the linear relationship derived from the arc spectra. By using the preliminary correlation for correcting the effect, it is possible to align the spectra within ~0.1 pixel or 120 m/s.

The UVES enclosure is thermally isolated. This has a damping effect on the external temperature variations and additionally the VLT enclosures are air-conditioned to minimize the day-night thermal excursions. The gradients of temperature in the UVES enclosure are typically less than 1 °C over 12 hours, apart from times of passage of a strong weather front. Depending on the type of

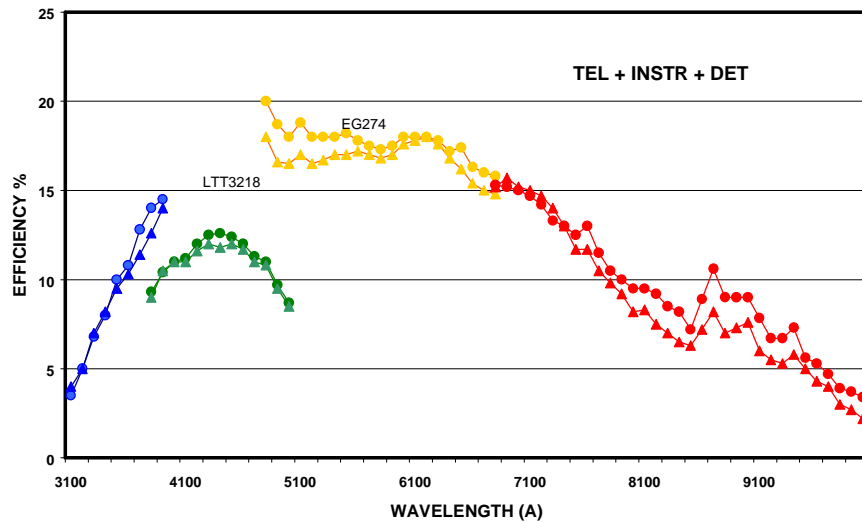
The shift of the spectra with temperature appears in first instance larger than expected by the variation in the spectral dispersion due to the change of the refraction index of air with temperature alone and suggests thermal effects on the mechanics as well. Arc spectra of the UVES standard formats are taken regularly by the ESO astronomers who operate the instrument. As this data base builds up, we plan to refine the model including the effect of atmospheric pressure and the thermal expansion of the echelle mount. It should then be possible to predict the positions of the lines as a function of temperature and pressure with an accuracy close to 50m/sec.

1.3 UVES efficiency

High efficiency over the whole spectral range (300-1100 nm) was one of the key requirements for the instrument. It led to the choice of two separate optical paths for the UV-Blue and the

each echelle order. Note the jump in efficiency at ~ 860 nm due to the higher red efficiency of the MIT/LL CCD with respect to the EEV. The observations were done in the spring of 2000, shortly after the re-aluminization of M1 and M3. To take out the contribution of the three reflections in the telescope the values should be multiplied on average by 1.4. An increase of $\sim 20\%$ was measured with respect to the measurements carried out in December when the mirror coatings were 1 year old. The difference between the two stars is very much indicative of the accuracy of the measurement. With these efficiencies and the collecting power of the 8.2m telescope, UVES at Kueyen has a place at the top in the league of the high resolution spectrographs at large telescopes worldwide.

Fig.5. The efficiency of UVES, including the telescope, as derived from two dichroic observations with wide slits of two standard stars. The four segments correspond to the spectral ranges of the four CDs, two for each arm. The raise at ~ 860 nm corresponds to the passage from the EEV to the MIT/LL CCD in the red arm mosaic.



The decrease in efficiency toward the extreme UV and the far red are due to the lower efficiencies of the CCDs and, to a lesser extent, of the CDs in these spectral range. There is the possibility of a factor of two improvement by retrofitting these components with optimized ones. The upgrade is technically straightforward. New CDs are on order and could be implemented within 2000.

Detective efficiency is the main parameter that measures the overall efficiency of the instrument in collecting scientific data. The size of the spectral range covered in a single exposure is the second one. The two standard settings of UVES with dichroics cover the spectral ranges 90nm ($\lambda_{\text{cen}}=346\text{nm}$) + 200 nm ($\lambda_{\text{cen}}=580\text{nm}$) and 100nm ($\lambda_{\text{cen}}=437\text{nm}$) + 400nm ($\lambda_{\text{cen}}=860\text{nm}$) in a single exposure respectively, and this without any spectral gaps in the red part of the spectrum apart from the 5-10 nm losses due to the space between the two CCDs in the mosaic. Finally, the density of information depends on the sampling in the spatial and dispersion directions in the spectra. At the typical UVES resolution of 50000 (corresponding to a slit width of $\sim 0.8''$) the spectral lines are sampled on average by 4 pixels in the blue arm and by 5 in the red. This large sampling is an advantage in the data reduction (e.g. in the rejection of radiation hits, to achieve very high S/N) and in the subsequent scientific analysis of the spectra.

2. HIGHLIGHTS OF THE FIRST SCIENTIFIC RESULTS

2.1. Introduction

In the three weeks of Commissioning following first light on September 27th, the instrument, the first to be installed at UT2, was successfully tested. The number of hours lost to hardware and software problems was less than 10. In view of this smooth operation of the instrument, an unusually large number of scientific observations was obtained in addition to the various operation and performance tests. 94 hours of these observations of stellar and extragalactic targets have been released in February 2000 by the VLT archive for public use. We report below on the scientific results from four different type of observations obtained to demonstrate: a) the unique UV efficiency of UVES (observations of the Beryllium lines

at ~ 313 nm and of the Lyman α forest in the range $z=1.5-2$); b) its high resolution and high signal-to-noise ratio capability (measurement of the Lithium isotope ratio) and c) high red efficiency (determination of the metal abundance in a damped system at $z=3.4$ from the observation of the $\lambda 202.6$ nm line of the undepleted Zn).

2.2. The Beryllium abundance in metal poor stars

Beryllium, together with lithium and boron, belongs to a small group of *light elements* which can be generated by a few physical processes only: thermonuclear reactions in the early universe, galactic cosmic-ray (GCR) spallation reactions,

Fig.6. The region of the Be II doublet of LP815-43($V=10.91$) and CD -24° 17504 ($V=12.18$) in the reduced UVES spectra with Be and the other main features marked. The dotted lines are preliminary synthetic spectra. The model for LP 815-43 was computed with a tentative beryllium abundance of $\log(\text{Be}/\text{H})+12 = -1.3$.

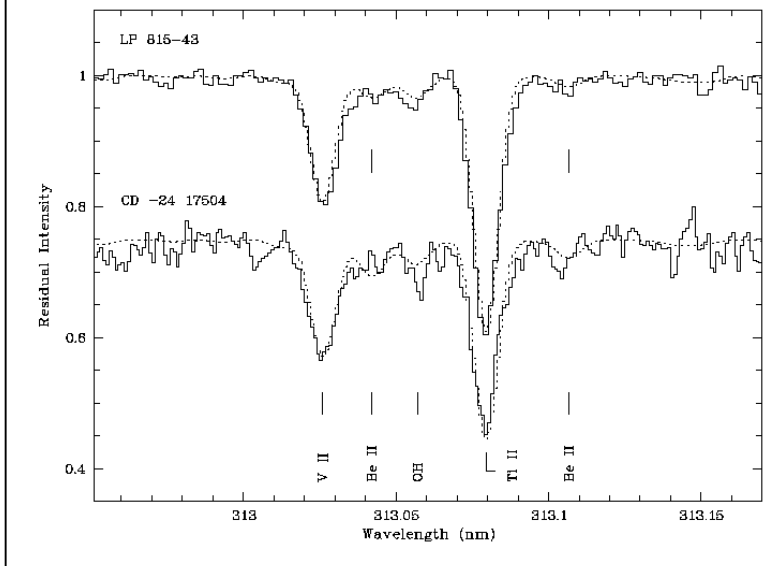
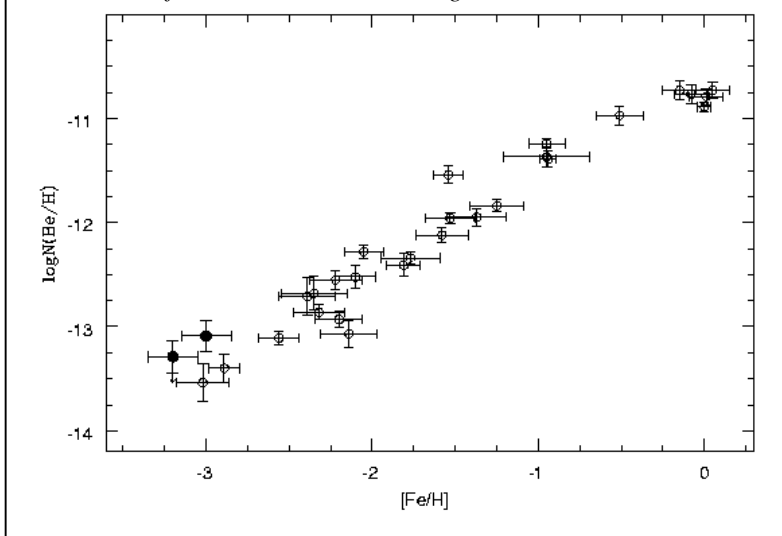


Fig.7. $\log N(\text{Be}/\text{H})$ vs $[\text{Fe}/\text{H}]$ for the highest quality data points currently available. Open circles are measurements from the work of Boesgaard et al (1999) at Keck whereas the filled circles are the observations from UVES Commissioning.



stellar processes during the Asymptotic Giant Branch (and possibly Red Giant Branch) phases and maybe ν -spallation in supernovae (still under debate). Beryllium has a special place in the general scheme of nucleosynthesis being the lightest stable nuclide not synthesized in the Big Bang. Together with ${}^6\text{Li}$ and ${}^{10}\text{B}$, it is considered a pure product of cosmic ray (CR) spallation nucleosynthesis, being generated by the bombardment in the interstellar medium of C, N and O nuclei by protons and α -particles.

The knowledge of the abundance of Be in the Galaxy allows to trace its chemical history, that of the cosmic rays and provides a further test of theories on big bang nucleosynthesis. The abundance of Be is obtained from the Be II resonant lines at 313.1 nm, near the atmospheric cut-off. The high atmospheric extinction and the usually low efficiency of instrumentation at this wavelength make measurements of the Beryllium line very difficult even in relatively bright objects. Among the most interesting target are faint metal-poor stars which have formed in the early phases of the galaxy evolution from low abundance interstellar gas and hence trace the pristine abundance of Be. So far, only two measurements exist of beryllium abundance in stars with $[\text{Fe}/\text{H}] \approx -3$ where $[\text{Fe}/\text{H}] = \log(\text{Fe}/\text{H}) - \log(\text{Fe}/\text{H})_{\text{solar}}$.

UVES will play an unique role in this area of research because its global efficiency at this wavelength is ~ 3 times better than the most powerful facility available so far, the HIRES spectrograph at the 10m Keck I telescope.

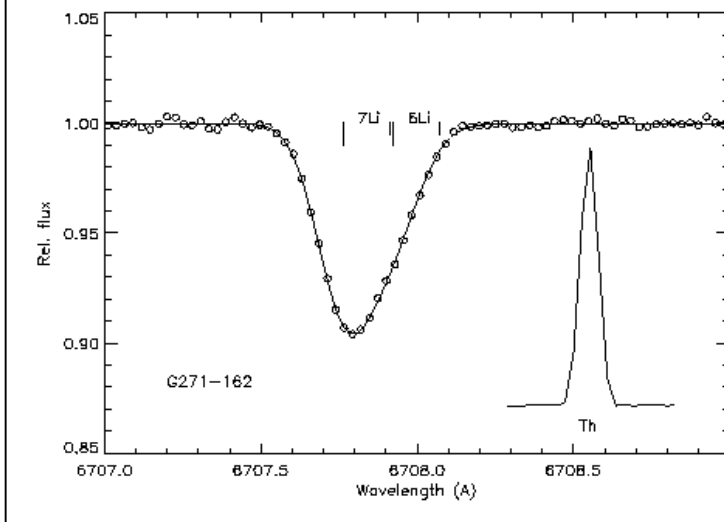
As an advance test two extremely metal-poor stars, LP 815-43 and CD-24°17504, with metallicity around -3.1 and -3.5 respectively, were observed during Commissioning. The exposure times have been of 3 hours for LP815-43 ($V=10.91$) and 2.5 hours for CD -24°17504 ($V=12.18$) and in the added up spectra a S/N around 100 was achieved for the first and around 80 for the second star at a resolving power of ≈ 45000 (see Fig. 6).

A 3σ detection of Be has been claimed in LP 815-43 whereas an upper limit has been set for CD -24° 17504 by Primas et al.⁵ The measured equivalent width of the bluer Be II line in LP 815-43 is $1.8 \pm 0.6 \text{ m\AA}$, which implies $\log(\text{Be}/\text{H})+12 = -1.09$. limit in the second star is set at $\log(\text{Be}/\text{H})+12 < -1.29$. These values are in agreement with previous determination of Be in stars of slightly higher metallicity. Figure 7 shows these 2 new UVES measurements obtained in a few hours of integration in the first three weeks of commissioning together with high quality data collected by Keck in the last six years. They demonstrate the potentiality of UVES to bring a decisive contribution in the understanding of the behaviour of Be abundance with metallicity.

2.3. The isotopic Lithium abundance in a metal-poor halo star

The isotopic abundances of lithium in metal poor stars (which have been formed from interstellar gas early in the life of the Universe, some 12-14 billion years ago) provide key information about the amount of Li made by nucleosynthesis in the Big Bang, and by reactions between cosmic rays and nuclei in the interstellar gas. To disentangle the relative contribution of these two processes, and to correct the measured abundances for Li depletion by thermonuclear reactions with protons at the bottom of the stellar convection zone, isotopic abundances are needed for a large sample of stars. In stellar spectra, the measure of the low abundance ^6Li are based on the increased width and asymmetry of the ^7Li 670.8nm doublet introduced by the isotope shift of ^6Li ($0.016\text{nm} = 7.1\text{km/s}$). It is a critical measurement which requires both high spectroscopic resolution and very high signal-to-noise ratios. The signature of ^6Li in stellar spectra has been recognized so far in four stars only two halo stars and in two metal-poor disk stars at a level of $^6\text{Li} / ^7\text{Li} = 0.05$.

Fig.8. 3-hr UVES spectrum of G271-162 in the Li line region. The open circles are the observed data and the full drawn line a model atmosphere synthesis with $^6\text{Li}/^7\text{Li} = 0.02$. The inserted profile of a nearby thorium line represents the instrumental profile. The Li line in G271-162 is considerably broader due to Doppler-broadening in the stellar atmosphere caused by thermal and gas-turbulent motions of the absorbing Li atoms. The line is also asymmetric due to the doublet structure of the ^7Li absorption (relative strength of the components 2:1. Any presence of ^6Li adds, however, to the asymmetry of the line.



summed up. The final S/N (see fig.8) of the reduced spectrum proves to be higher than 600 (see fig.8). The data have been discussed in Nissen et al.⁶ When compared with the spectra from detailed model atmospheres the observed profile of the Li I 670.8 line reveals a possible detection of ^6Li , corresponding to a $^6\text{Li}/^7\text{Li} = 0.02$, a relatively low value with respect to previous stellar determinations and to the 0.08 value measured on Earth and in meteorites. This result proves the need to extend the survey to a large number of stars before the value of the isotope ratio and its scatter is well understood and the ratio be used as a cosmological parameter.

UVES at Kueyen is potentially capable to extend these observations to fainter stars and a wide range of metallicities and hence to make a very significant contribution to our understanding of the formation of the light elements in the Universe and their cosmic chemical evolution. On the technical side, this program is a critical test of the instrument spectrophotometric calibration. Flat-fielding procedures must provide a very accurate correction of the pixel to pixel variations in the detector (which can be up to 20% at red wavelengths) in order to reach signal-to-noise ratios in the detected stellar continuum higher than 400, as needed for this type of observations.

The observations of the metal-poor ($[\text{Fe}/\text{H}] = -2.2$) halo star G271-162 ($V=10.35$) at a $112000 \Delta\lambda/\lambda$ resolution were included in the Commissioning program to prove this capability of UVES. The star represents a group of about 50 halo turn-off stars which are too faint to be studied using high resolution spectrograph at 4m class telescopes. A total of around 3 hrs of integration obtained in excellent seeing through a slit open to 0.3 arcsec were

2.4. The intergalactic medium in the redshift interval $z=1.5-2$

The physical state of the intergalactic medium (IGM) at high redshift is important to understand the formation and evolution of large scale structures and individual galaxies which mostly form early in the life of the universe. The absorption line

Fig.9. This part of the normalized UV spectrum of the $z=2.4$ QSO HE22-28 illustrates the final quality of the reduced data from UVES. The resolution is ~ 40000 . Most of the lines are due to Ly alpha clouds at redshifts in the little-studied interval $z=1.9-2.1$

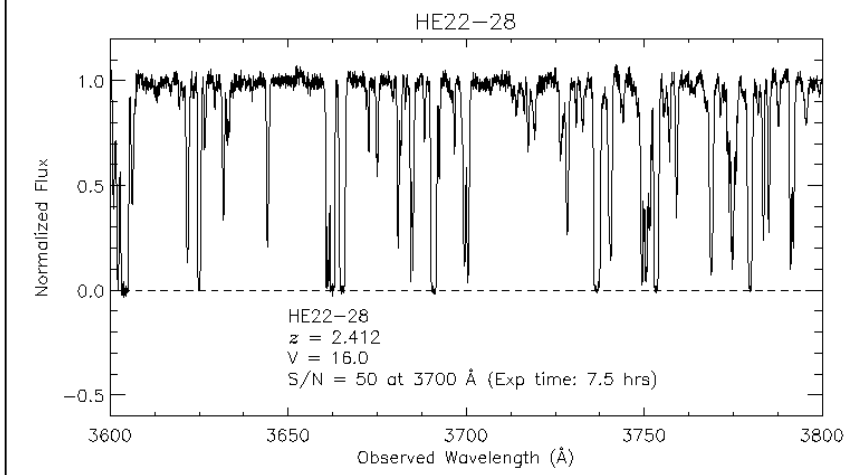
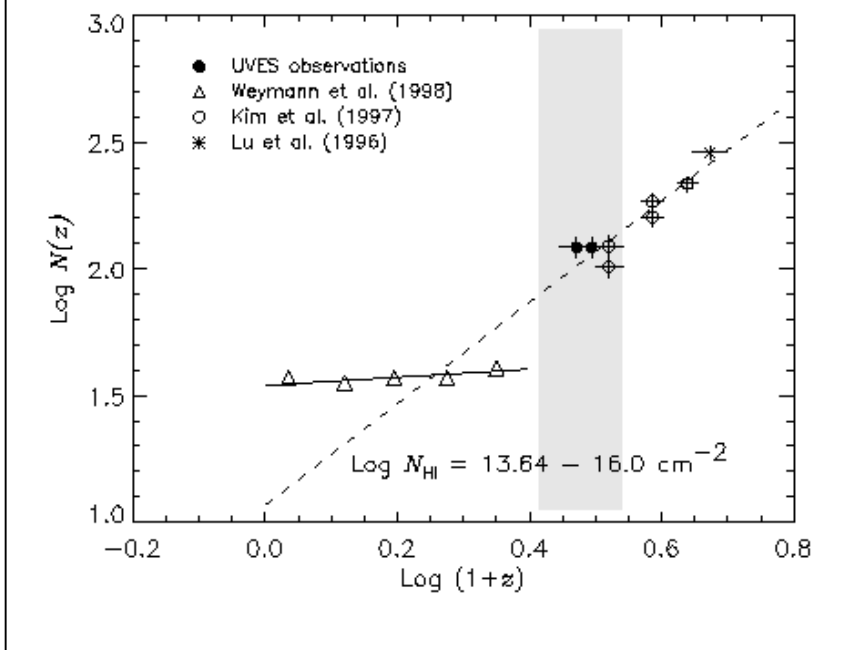


Fig.10. The number density evolution of the Ly alpha lines with z to the limit of the existing HST observations at lower redshift ($N(\text{HI}) = 10^{(13.64 - 16)} \text{ cm}^{-2}$). The filled symbols are the estimates from the HE22-28 (average $z = 2.12$) and the J2233-606 ($z = 1.96$) UVES spectra. Open circles and stars are existing measurements from Keck, open triangles measurements at redshift $z < 1.5$ obtained at lower spectroscopic resolution with the HST (open triangles).



systems imprinted in the spectra of high- z QSOs at all redshifts shorter than the Ly alpha emission of the QSO, provide a unique and powerful tool to study the IGM in the Universe up to $z \sim 5$. In particular, the Ly alpha forest, absorption line systems with $N(\text{HI})$ less than around 10^{16} atoms cm^{-2} , is important since it is thought to be composed by gas systems which lie close to the mean baryon density in the IGM and are still in the regime where the linear approximation in the study of the physics of the gas can be applied. The properties of the Ly alpha forest at different redshifts constrain the cosmological parameters such as the baryon density and the density parameter Ω , and current cosmological theories on the evolution of the early universe.

The Ly α forest and the metal systems (Ly alpha absorptions of higher column density to which many metal lines are also associated) are thought to be photoionized by the metagalactic UV background and enriched by the metals produced by the first generations of stars. As such, they also provide a unique opportunity to probe the intensity and shape of the metagalactic UV background as well as the star formation scenarios which can account for the observed metal abundances.

The epoch in the universe corresponding to redshifts between 1.5 and 2.5 (see grey band in Fig.10) is one of the most interesting because it is characterised by intense star formation. It remains however largely unstudied because the line "signatures" of luminous matter at these redshifts (both stars and emitting gas) fall mainly in the little-studied IR region and the key resonance absorption lines of the gas in the UV region of the spectrum where no efficient high resolution spectrograph was yet in operation at very large telescopes. The relatively high UV efficiency of UVES

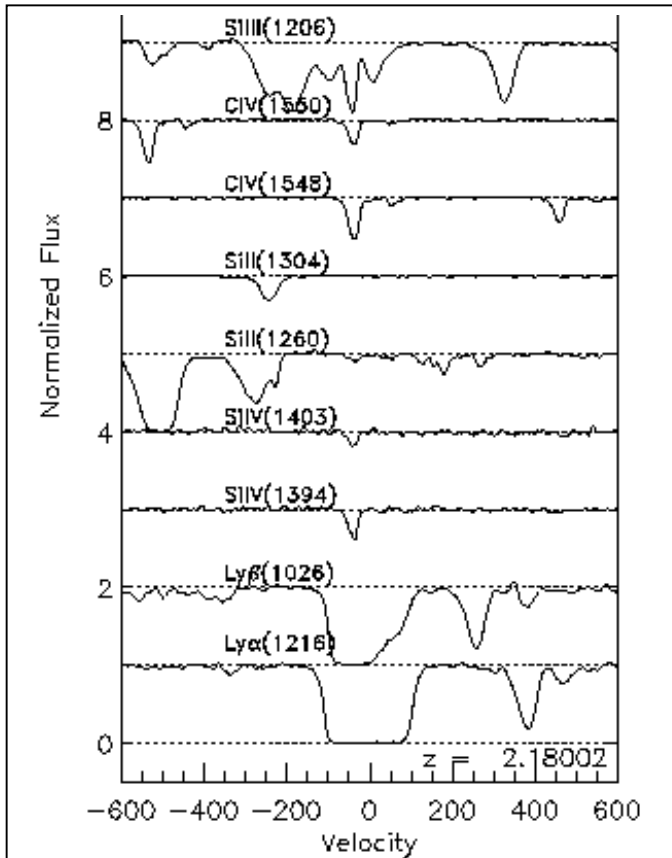
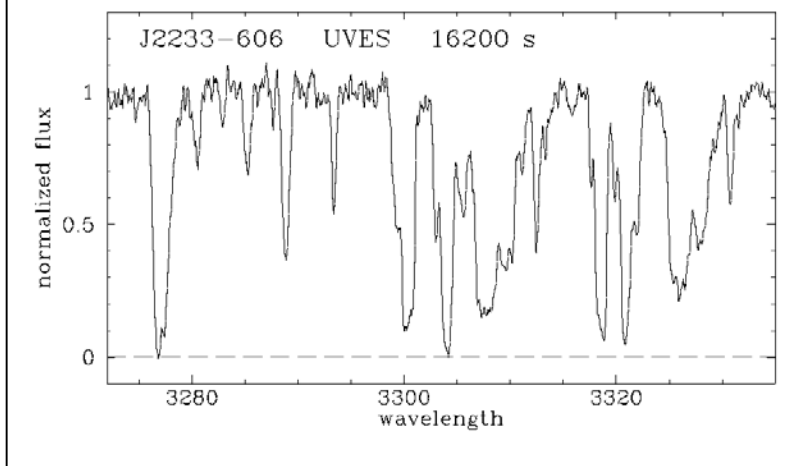


Fig.11. Lines from a metal-line system at $z=2.18$ towards HE22-28.

Fig.12. Part of the UVES spectrum of J2233 -606 in the Lyman α forest at redshift $z \sim 1.7$. The resolving power is 45000.



Facility for the HST (<http://stecf.org/hstprogrammes/J22>). With an average resolution of 45000 (~ 6.5 km/sec) and a S/N ratio in the range 40-80, the spectrum is of unique quality (Fig.12) and will permit a detailed study of the properties of Lyman alpha forest and of the metal systems, including their ionization state and abundances. For the first time, astronomers have at their disposal high quality data to establish a relationship between the luminous matter (galaxies) and the absorbers, both in the QSO environment and at various redshifts along the line of sight to the QSO.

opens new possibilities of research in this field and already during commissioning, QSOs at redshifts around 2 were extensively observed and the data are now available from the ESO archive. The analysis on the forest and on the metal absorption systems (Kim et al.⁷) gives the first detailed information on the Intergalactic Medium in this redshift range (see figures 9,10 and 11). Concerning the number density evolution UVES results are in satisfactory agreement with earlier Keck measurements at higher redshift, resulting in a linear relation $dN/dz = 11.75 (1+z)^{2.01}$ while a discrepancy is observed with the measurements at redshift $z < 1.5$ obtained at lower spectroscopic resolution with the HST. The spectrum of one metal system at $z=2.18$ (Fig.11) illustrates the advantage of the observations in the far UV to explore systems at this intermediate redshift. Although the Ly alpha absorption line shows only one component, with the metal lines blue-shifted by ~ 40 km/sec, the corresponding Ly beta line (observed $\lambda = 326$ nm !) reveals that the complex consists of two components at $z=2.1795$ and at $z=2.1804$. The Voigt profile fitting give a total column density of $N(\text{HI}) = 1.3 \times 10^{16} \text{ cm}^{-2}$ and accurate values for the column densities of SiIV, SiII, CIV, SiIII and CII. The SiIV/CIV ratio, an indicator of the temperature of the ionizing background (see Songaila, 1998, AJ,115,2184) for the $z=2.1795$ component gives ~ 0.23 which is similar to what found in higher z systems, suggesting little evolution in the shape of the spectrum of the ionizing background.

A special case of observations during Commissioning was the $m(v)=17.5$ quasar J2233-606 with an emission redshift

$z=2.238$. The QSO sits at the center of the Hubble Deep Field South (HDF-S), a region of the sky in which the Hubble Space Telescope has provided the deepest images ever taken at wavelengths from the UV to the infrared. The photometric information on the galaxies in this field, complemented by low resolution spectroscopy on the brightest ones, is being used to reconstruct the distribution of luminous matter with redshift. The UV spectrum of the QSO has been already observed by the STIS instrument of the HST while 4-m class telescopes have been used to get high resolution spectra at blue-visual and red wavelengths. UVES has observed the complete spectrum of the QSO in the range 305-1000 nm for a total integration time of ~ 28500 second. The data are available in the web pages of the European Coordinating

2.5. First crucial measurements of Zinc in a damped system at $z>3$

Damped Lyman α systems (DLA) are the class of QSO absorption systems showing the largest gas column density ($N(\text{HI}) > 2 \times 10^{20} \text{ cm}^{-2}$) and are widely believed to be the progenitors of the present-day galaxies. They are associated with

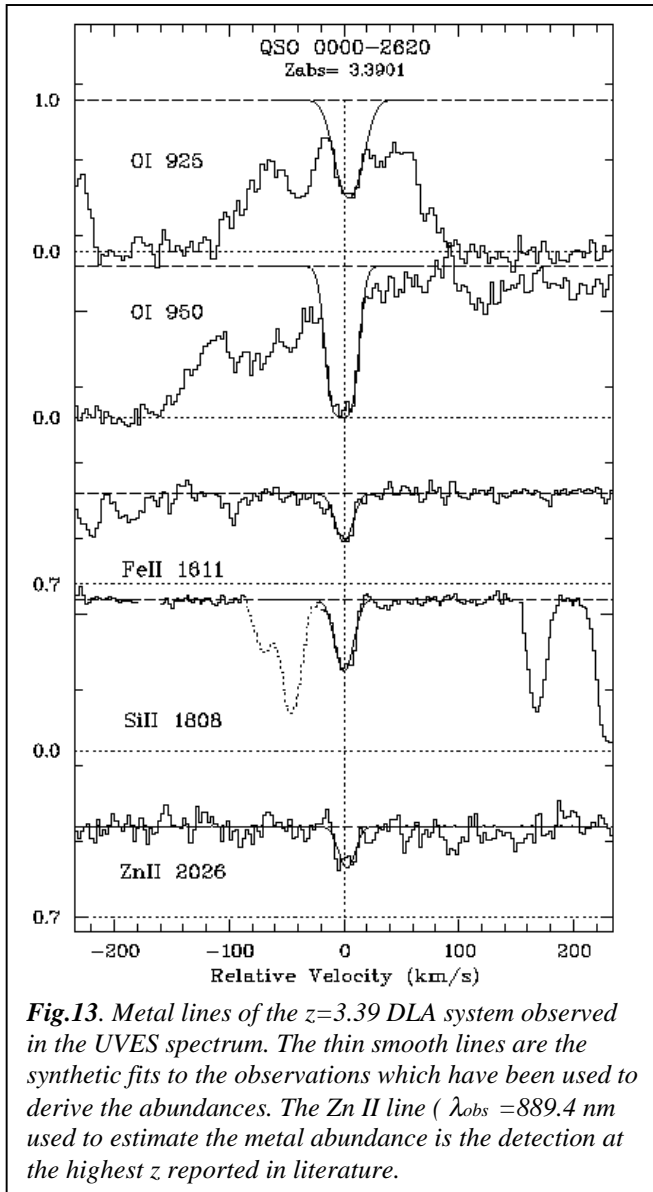


Fig.13. Metal lines of the $z=3.39$ DLA system observed in the UVES spectrum. The thin smooth lines are the synthetic fits to the observations which have been used to derive the abundances. The Zn II line ($\lambda_{\text{obs}} = 889.4 \text{ nm}$) used to estimate the metal abundance is the detection at the highest z reported in literature.

the majority of the neutral gas at high redshifts. By studying the low ionization metal absorption lines associated to the damped, the absolute and relative abundances of several key elements can be measured. They reveal the amount of nuclear processing which has taken place in these systems and the dominant processes. The abundance measurements at high redshift are the most accurate estimates of metal abundances we have for galaxies in the early stage of galaxy formation in the Universe.

As a test of the capability of UVES in this field of research the quasar 0000-2620 ($V=17.5$, $z(\text{em})=4.1$) was observed in the spectral regions 370-500 nm and 660-1000 nm to study the absorption lines from a DLA at $z(\text{abs})=3.3901$, one of the highest redshift known for these systems. It corresponds to an age of $2-3 \times 10^9$ years, or less than 20% of the Universe age. The system has been already studied with instruments at 4m telescopes and at Keck, but the high VLT-UVES throughput in the blue and in the far red have provided a spectrum with unique new information.

The 12500s exposure has lead to the first detection of the Zn II 2026.136 Å transition redshifted at 8895 Å yielding an abundance of $[\text{Zn}/\text{H}]=-2.06$, when a $N(\text{HI})=2.6 \times 10^{21}$ is assumed, showing that the object has a very low abundance and confirming that the galaxy is in the early stages of its chemical evolution (see Molaro et al.⁸) Compared with the larger abundances observed in the DLA galaxies at lower redshift it provides a first hint for a cosmological chemical evolution with abundances decreasing with the increasing of redshifts.

The abundances of Cr and Fe are also obtained and found close to those of the Zn. The coincidence in the abundances between refractory and non-refractory elements suggest that dust is not yet formed in this protogalaxy. At the high redshift of this damped system the O I 925 and 950 Å oxygen lines are visible although falling within the Lyman alpha forest shortward of the QSO Ly α emission (see figure). These lines have line strengths much smaller than the O I 1302 Å line, which is strongly saturated, and allow for the first time a rather accurate measurement of the oxygen abundance in a DLA at $[\text{O}/\text{H}]=-1.85$. The pattern of

relative abundance of the alpha elements like O, S, and Si with respect to iron-peak elements like Zn, Fe and Cr which emerges for this DLA suggests a model of galaxy evolution characterised by episodic or low star formation rate rather than a Milky-Way-type evolutionary model.

ACKNOWLEDGEMENTS

We are greatly indebted to all the people involved in the conception, construction and commissioning of UVES for the unique performance of the instrument from the first night of observations. We thank Paolo Molaro (Observatory of Trieste)

and Poul E. Nissen (University of Aarhus) for permission to quote their results based on UVES spectra in advance of publication and C. Ledoux for measuring the shift of the sky lines in the spectra.

REFERENCES

1. H. Dekker, S. D'Odorico, A. Kaufer, B. Delabre and H. Kotzlwski, " Design, construction and performance of UVES, the echelle spectrograph for the UT2 Kueyen telescope at the ESO Paranal Observatory", Proc. SPIE 4008, (in print),
2. R. Dorn, C. Cavadore, J. Beletic, J.L. Lizon, "Design, construction, and operating parameters of the CCD systems for the blue and red arms of UVES: the Echelle Spectrograph for the UT2 Kuyen Telescope at the ESO Paranal Observatory", *Proc. SPIE 4008 (in print)*, 2000
3. A. Longinotti, P. Dimarcantonio and P. Santin, "UVES Instrument Software in the VLT Environment", *Proc. SPIE 4009 (in print)*, 2000
4. Ballester, P. Grosbol, K. Banse, A. Disaro, D. Dorigo, A. Modigliani, J.A. Pizarro De La Iglesia, O. Boitquin, "Quality Control System for the Very large Telescope", *Proc. SPIE 4010 (in print)*, 2000
5. F. Primas, P. Molaro, P. Bonifacio and V. Hill, "First UVES Observations of Beryllium in Very Metal-Poor Stars", A & A., submitted, 2000
6. P.E. Nissen, M. Asplund, V. Hill and S. D'Odorico, " The Lithium isotope ratio in the metal-poor star G271-162 from VLT/UVES observations", A. & A., in press, 2000
7. T. Kim, S. Cristiani and S. D'Odorico, in preparation, 2000
8. P. Molaro, P. Bonifacio, M. Centurion, S. D'Odorico, G. Vladilo, P. Santin and P. Dimarcantonio, "UVES observations of QSO 0000-2620: oxygen and zinc abundances in the Damped Ly α galaxy at $z_{\text{abs}} = 3.3901$ " Ap.J. in press, 2000